ELECTRONIC AND OPTICAL PROPERTIES OF M_{13} AND $M_{12}Cr$ (M = Cu, Ag, and Au) CLUSTERS: A COMPARATIVE DFT INVESTIGATION

Nguyen Van Dang[1], Vi Tien Thanh[1], Nguyen Thi Mai[2], Nguyen Thi Dung[1], Phan Thanh Phuong[1], Tran Xuan Quy[1], Le Thi Tuyet Ngan[3], Nguyen Thanh Tung[2], Ngo Thi Lan[1*]

[1]TNU - University of Sciences, [2]Institute of Materials Science - Vietnam Academy of Science and Technology

[3]TNU - University of Information and Communication Technology

ARTICLE INFO

Received: 25/4/2025

Revised: 28/5/2025

Published: 28/5/2025

KEYWORDS

Metal clusters

Optical properties

Infrared spectroscopy

Density functional theory

Absorption spectra

ABSTRACT

Nanoclusters have recently emerged as promising building blocks with potential applications in advanced nanostructured materials, owing to their unique catalytic, magnetic, and electronic properties. This work compared the infrared spectra and absorption spectra of the ground-state structures M_{13} and $M_{12}Cr$ (M = Cu, Ag, and Au) clusters using density functional theory and time-dependent density functional theory approaches. Specifically, we employed the BP86 functional combined with cc-pVTZ-pp and cc-pVTZ basis sets for M and Cr atoms, respectively. Chromium (Cr) dopant atom has five unpaired valence electrons, with an outermost shell configuration of $3d^5 4s^1$. These valence electrons exhibit high mobility, allowing them to move freely and form a delocalized electron cloud for clusters. In contrast, the remaining electrons that do not participate in forming the delocalized electron cloud localize in the *d*-Cr, resulting in significant differences in the characteristics of IR vibrational modes for M_{13} and $M_{12}Cr$ clusters. The absorption spectra analysis revealed no absorption signals for $Ag_{12}Cr$ and $Cu_{12}Cr$ clusters, while $Au_{12}Cr$ cluster exhibits a notable absorption peak at 1270 nm (0.976 eV). These findings provide valuable insights into the vibrational and optical characteristics, establishing a foundation for further theoretical and experimental investigations.

CẤU TRÚC ĐIỆN TỬ VÀ TÍNH CHẤT QUANG CỦA CỤM NGUYÊN TỬ M_{13} VÀ $M_{12}Cr$ (M = Cu, Ag, và Au): NGHIÊN CỨU SO SÁNH SỬ DỤNG PHƯƠNG PHÁP PHIẾM HÀM MẬT ĐỘ

Nguyễn Văn Đăng[1], Vi Tiến Thành[1], Nguyễn Thị Mai[2], Nguyễn Thị Dung[1], Phan Thanh Phương[1], Trần Xuân Quý[1], Lê Thị Tuyết Ngân[3], Nguyễn Thanh Tùng[2], Ngô Thị Lan[1*]

[1]Trường Đại học Khoa học - ĐH Thái Nguyên, [2]Viện Khoa học Vật liệu - Viện Hàn lâm Khoa học và Công nghệ Việt Nam

[3]Trường Đại học Công nghệ Thông tin và Truyền thông - ĐH Thái Nguyên

THÔNG TIN BÀI BÁO

Ngày nhận bài: 25/4/2025

Ngày hoàn thiện: 28/5/2025

Ngày đăng: 28/5/2025

TỪ KHÓA

Cụm nguyên tử kim loại

Tính chất quang

Phổ hồng ngoại

Phương pháp phiếm hàm mật độ

Quang phổ hấp thụ

TÓM TẮT

Cụm nguyên tử gần đây nổi lên như những viên gạch đầu tiên hứa hẹn tiềm năng ứng dụng cho các vật liệu cấu trúc nano tiên tiến nhờ vào tính chất xúc tác, từ tính và điện tử thú vị. Nghiên cứu này so sánh phổ hồng ngoại và phổ hấp thụ phân tử của các cấu trúc M_{13} và $M_{12}Cr$ (M = Cu, Ag và Au) ở trạng thái cơ bản sử dụng phương pháp phiếm hàm mật độ và phiếm hàm mật độ phụ thuộc thời gian. Cụ thể, chúng tôi sử dụng phiếm hàm BP86 kết hợp với bộ hàm cơ sở cc-pVTZ-pp và cc-pVTZ áp dụng lần lượt cho nguyên tử M và Cr. Nguyên tử pha tạp Cr có năm điện tử hóa trị chưa ghép cặp tương ứng với cấu hình điện tử phân lớp ngoài cùng $3d^5 4s^1$. Những điện tử hóa trị này có tính linh động cao, do đó chúng dễ dàng di chuyển và hình thành đám mây điện tử tự do cho cụm nguyên tử. Ngược lại, các điện tử còn lại không tham gia vào hình thành đám mây điện tử tự do của cụm nguyên tử sẽ định xứ trên orbital *d*-Cr, kết quả có sự khác biệt đáng kể trong các mode dao động đặc trưng của cụm nguyên tử M_{13} và $M_{12}Cr$. Phân tích phổ hấp thụ phân tử cho thấy không thu được tín hiệu hấp thụ đối với cụm nguyên tử $Ag_{12}Cr$ và $Cu_{12}Cr$, trong khi $Au_{12}Cr$ thu được một đỉnh phổ rõ rệt tại bước sóng 1270 nm (0,976 eV). Những phát hiện này cung cấp những hiểu biết có giá trị về các đặc trưng dao động và đặc trưng quang học của cụm nguyên tử, tạo nền tảng cho các nghiên cứu lý thuyết và thực nghiệm trong tương lai.

DOI: https://doi.org/10.34238/tnu-jst.12674

* Corresponding author. *Email: lannt@tnus.edu.vn*

1. Introduction

Metal clusters have recently become an intriguing research subject due to their extensive application potential, which are regarded as foundational elements in the development of advanced nanostructured materials with remarkable chemical and physical properties [1] - [4]. Notably, the doping of transition metal atoms into metal clusters can significantly modify geometric structure, resulting in alterations to their electronic properties. Studies have highlighted that these modifications significantly impact the spin magnetic moment and the stability of the clusters [5] - [11]. Furthermore, alternations in both geometric and electronic structures are essential in determining the optical properties and catalytic capabilities of the clusters [12] - [16]. Consequently, the selection of appropriate doping atoms provides scientists with the ability to manipulate the optical characteristics of clusters effectively. For example, Y.S. Yu et al. [12] demonstrated that the adsorption capacity of Ag_nCr for CO is significantly higher than that of Cr atom. The optical spectra of Ag-Co clusters generally show minor variations in energy as the number of atoms increase [17]. The absorption peaks exhibit a clear redshift as the size of Cu atoms increase, as observed when comparing the absorption spectra of Ag_{13}^+, $Ag_{12}Cu^+$, and Cu_{13}^+ clusters [18]. This phenomenon is attributed to the increased activity of silver atoms in the outermost layer of the $Ag_{12}Cu$ cluster compared to those in Ag_{13} and Cu_{13} clusters. Another example is the impact Pd atom doping, which alters the structure and optical absorption properties of gold clusters [19]. While the structures of pure gold clusters have a planar (2D) structure, the Pd-doped gold clusters show stability in a 3D shape. Comparison of the infrared absorption spectra of pure Au_n^+ and doped Au_nPd^+ clusters demonstrates significant differences. Quantum calculations using the density functional method indicate that these changes correlate with shifts in electron density. The intensity of oscillations during the optical transition process significantly decreases when Pd is doped into Au_4^+ and Au_4^+Ar clusters. The quenching effect observed in $PdAu_3^+$ clusters results from structural changes induced by Pd doping, alongside alterations in the electronic structure of the atomic clusters.

Although studies have examined the optical properties of the Cu_n, Ag_n, and Au_n alloy clusters, none have systematically clarified the relationship between geometric structure, electronic configuration, and their optical properties, particularly for metal clusters doped with transition metal atoms. To address this issue, we analyze and compare the vibrational infrared spectra/adsorption peaks of the most stable structures of pure M_{13} and doped $M_{12}Cr$ (M = Cu, Ag, and Au) clusters using the density functional theory (DFT) and time-dependent density functional theory (TD-DFT). This research aims to provide a valuable insight into the connections between the vibrational infrared spectra, UV-Vis spectra, the ground-state structures, and electronic configuration. Furthermore, these findings provide strong guidelines for future experimental investigations.

2. Methods

The geometric and electronic structures of $M_{12}Cr$ (M = Cu, Ag, and Au) clusters were carried out by density functional theory (DFT) calculations in the Gaussian 09 package [20], [21]. The structures were optimized using BP86 functional combined with cc-pVDZ-pp and cc-pVDZ basis sets for M and Cr atoms, respectively. Isomers with relative energies below 2.0 eV were considered for further calculations. These selected isomers underwent single-point energy calculations using the same functional but with larger basis sets, specifically cc-pVTZ-pp for M atoms and cc-pVTZ for Cr atom, based on previous investigations [5], [6]. The reliability of the current computational scheme has been verified through comparison with earlier calculations on metal and chromium dimers. Our results are summarized in Table 1, showing alignment with experimental data. Following the optimization calculations, we performed additional frequency evaluations to identify the lowest-structure for the cluster. Furthermore, the UV-Vis spectrum and its associated electronic transitions were determined using the time-dependent density functional theory (TD-DFT) method.

Table 1. *The dissociation energies (DE, eV) of ground state M-Cr and M_2 (M = Cu, Ag, and Au) dimers*

Dimers	DE, eV		References
	Cal.	Expt.	
Cu-Cu	2.01	2.01 ± 0.08	[22]
Cu-Cr	1.70	1.61 ± 0.22	[23]
Ag-Ag	1.62	1.63 ± 0.03	[23]
Ag-Cr	2.56	2.80	[24]
Au-Au	2.27	2.29 ± 0.30	[23]
Au-Cr	2.27	2.28 ± 0.30	[23]

3. Results

3.1. Structure and spin multiplicities

The stable geometric structure of M_{13} (M = Cu, Ag, and Au) clusters was optimized using the density functional theory approach at the BP86/cc-pVTZ-pp level. In this studies, we obtained numerous geometric structures corresponding to low-energy spin states, ensuring the absence of negative frequency values. The most stable geometric structure of M_{13} was determined by evaluating the relative energy of different isomers. Following this, a transition metal atom Cr was substituted at all feasible positions within the most stable M_{13} clusters. This resulting structure was used as the input structure for subsequent calculations. The BP86 functional in conjunction with the cc-pVTZ-pp and cc-pVTZ basis sets was utilized the metal atoms (Cu, Ag, and Au) and the transition metal atom Cr, respectively. Among the numerous isomers obtained, only those with the lowest energy were selected for further investigation. The results are presented in Figure 1.

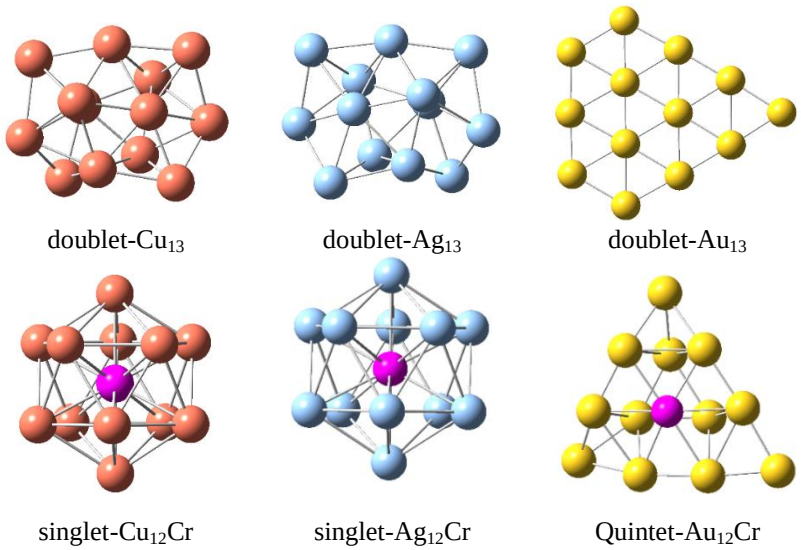

Figure 1. *Optimized structures and spin multiplicities of the lowest lying isomers M_{13} and $M_{12}Cr$ (M = Cu, Ag, and Au). The red, light blue, yellow, and pink balls show Cu, Ag, Au, and Cr, respectively*

At first glance, significant differences are observed in the geometric structure and and spin multiplicities of M_{13} clusters compared to $M_{12}Cr$ (M = Cu, Ag, and Au) clusters, suggesting that the transition metal atoms significantly influence both the geometric structure and electronic configuration of the metal clusters. Specifically, the global structure of the doublet Cu_{13} and doublet Ag_{13} atomic clusters prefers a cage-like (3D) arrangement, whereas the doublet Au_{13} cluster has a planar (2D) structure. While we doped exactly the same dopant (Cr atom), there are two main differences between the host systems. First, $Cu_{12}Cr$ and $Ag_{12}Cr$ clusters exhibit a perfect icosahedral structure with singlet states, in which the Cr atom is located at the center of the icosahedron. Second, the geometry of quintet $Au_{12}Cr$ cluster is a cone-like shape with Cr

located at the center of the face. This observation aligns well with earlier research findings [6], [12], [15], [25]. Owning to their icosahedral and cone-like shape geometries, $Cu_{12}Cr/Ag_{12}Cr$ and $Au_{12}Cr$ clusters exhibit slightly different molecular shell of electrons, respectively [6]. Chromium (Cr) dopant atom has five unpaired valence electrons, with an outermost shell configuration of $3d^5 4s^1$. Assuming that each copper, silver, or gold atom delocalizes one $4s^1$, $5s^1$, or $6s^1$ electron, $Cu_{12}Cr$, $Ag_{12}Cr$ and $Au_{12}Cr$ clusters provides a total of 18 valence electrons. For $Cu_{12}Cr/Ag_{12}Cr$ all $3d^5 4s^1$ valence of Cr delocalizes and joins with *s* valence electrons of the Cu_{12} and Ag_{12} host, resulting in the completely filling of the $1S^2 1P^6 1D^{10}$ to form a closed shell and stable structure with icosahedral singlet. By contrast, for $Au_{12}Cr$, only two delocalized electrons (one of 4*s*-Cr and one of 3*d*-Cr) join in twelve electrons of the Au host cluster, forming an electronic shell structure of $1S^2 1P^6 1D^6$. The remaining 4 electrons are localized on 3*d*-Cr atomic orbitals, resulting in an electronic configuration of $1S^2 1P^6 1D^6 3d^4_{\uparrow}$, responding to the cone-like structure quintet. In other words, this phenomenon of geometric transformation and spin multiplicities can be attributed to the electronic configuration of Cr dopant atom with five unpaired electrons of $3d^5 4s^1$. These valence electrons determine the tendency to occupy the Cr atom at the highest coordination numbers with the cluster hosts.

3.2. Stability

Relative stability is often considered an important parameter in evaluating the existence and properties of clusters. In this study, the influence of the transition metal atom (Cr) on the stability of the doped $M_{12}Cr$ clusters was examined by comparing them to their pure counterparts, using binding energy per atom (BE). In general, the BE is defined as the average difference between the energy sum of all the free atoms constituting the cluster and the total energy of the cluster, calculated as follows:

$$BE(CrM_n) = \frac{1}{n+1}[(E(Cr) + nE(M)) - E(CrM_n)] \quad (1)$$

$$BE(M_{n+1}) = \frac{1}{n+1}[(n+1)E(M) - E(M_{n+1})] \quad (2)$$

Where E(Cr), E(M), $E(CrM_n)$, and $E(M_{n+1})$ are the total electron energies of the most stable atoms and Cr, M, CrM_n, and M_{n+1} (M = Cu, Ag, and Au) clusters, respectively.

Table 2. *Binding energy per atom (BE, eV) and dissociation energy (DE, eV) of M_{13} and $M_{12}Cr$ (M = Cu, Ag, and Au) clusters correspond to the two decay channels: loss of a M atom and loss of a Cr atom*

Clusters	Binding energy (BE, eV)	Dissociation energy (DE, eV)	
		Loss M	Loss Cr
Cu_{13}	2.24	2.69	-
$Cu_{12}Cr$	2.35	3.37	3.88
Ag_{13}	1.59	1.76	-
$Ag_{12}Cr$	1.73	2.30	3.67
Au_{13}	2.06	1.89	-
$Au_{12}Cr$	2.13	2.40	2.26

The calculated BE results for M_{13} and $M_{12}Cr$ clusters are shown in Table 1. It can be seen that the BE of the doped $M_{12}Cr$ clusters is generally higher than that of the pure M_{13} clusters, suggesting that the substitution of a metal atom by a transition metal atom enhances the stability of clusters. This picture aligns with the observed trend of enhanced stability in Au_{19}/Au_9M^{2+} (M represents 3*d* transition metals) compared to Au_{20}/Au_{10}^{2+} clusters [5], [7], [8]. R. Xiong et al. [9] has shown that the substitution of a V atom for an Ag atom in Ag_{n+1} ($n \geq 2$) clusters can evidently enhance the stability of the host clusters. Notably, the BE of $Cu_{12}Cr$ cluster is the highest among the studied clusters at 2.35 eV. This result is fully consistent with previous research on the stability of the $M_{12}Cr$ clusters, particularly that $Cu_{12}Cr$ can be considered a potential superatom [6].

Analyzing the stability of clusters allows for the identification or creation of chemically inert species with specific properties, forming a foundation for developing advanced nanomaterials. It is important to note that the BE does not reflect the intrinsic stability of clusters, as the number and type of bonds vary for each atom. Therefore, the dissociation energy serves as a crucial parameter for evaluating the intrinsic stability of atomic clusters [26] - [28]. In this study, we compute the dissociation energy of pure clusters M_{13} and doped clusters $M_{12}Cr$ through two possible dissociation channels: the loss of a Cr atom and a M atom, according to the equation following.

$$DE(M) = E(M_n) + E(M) - E(M_{n+1}) \quad (3)$$

$$DE(Cr) = E(M_n) + E(Cr) - E(M_nCr) \quad (4)$$

$$DE(M) = E(M_{n-1}Cr) + E(M) - E(M_nCr) \quad (5)$$

In which, E(M), E(Cr), $E(M_n)$, $E(M_{n+1})$, $E(M_{n-1}Cr)$, and $E(M_nCr)$ are the total energies of the stable isomers of the atoms and clusters. Table 1 displays the findings of the dissociation energy calculations for M_{13} and $M_{12}Cr$ clusters. Compared to the pure clusters Cu_{13} (2.69 eV), Ag_{13} (1.76 eV), and Au_{13} (1.89 eV), the dissociation energy values of doped clusters $Cu_{12}Cr$ (3.37 eV), $Ag_{12}Cr$ (2.30 eV), and $Au_{12}Cr$ (2.40 eV) are significantly higher, respectively. This further supports the notion that the presence of transition metal atoms enhances the stability of the doped clusters. With the exception of the $Au_{12}Cr$ species, the dissociation channel of a metal atom is energetically preferred for the doped clusters compared to the dissociation channel of a transition metal atom Cr. This observation aligns consistently with the perfect icosahedron structure, in which the Cr atom is encapsulated by 12 metal atoms in the $Cu_{12}Cr$ and $Ag_{12}Cr$ clusters. In contrast, for $Au_{12}Cr$, the Cr atom prefers to occupy a face-centered position, as previously discussed. Notably, both dissociation channels (loss M and loss Cr) of the $Cu_{12}Cr$ cluster have higher values than those of other doped atomic clusters, further agreeing that the $Cu_{12}Cr$ cluster can be considered a potential superatom.

3.3. Electronic and optical properties

Infrared (IR) spectroscopy operates based on the phenomena of absorption, emission, or reflection of infrared radiation, transforming it into molecular vibrations. The IR spectrum is related to the vibrations or rotational movements that change the dipole moment. It is also associated with the curvature of the relationship between potential and distance between atoms. These vibrational modes also provide valuable insight into the structural properties and behavior of clusters, offering a deeper understanding of their molecular dynamics, chemical bonding and catalyze interactions. In this study, the effect of the transition metal atom (Cr) on the IR spectra of pure metal clusters M_{13} (M = Cu, Ag, and Au) and $M_{12}Cr$ clusters was conducted by the density functional theory (DFT) approach. The results are presented in Figure 2. The initial analysis of the IR spectra depicted in Figure 2 reveals that most of the observed spectral peaks are within the frequency range from 0-400 cm^{-1} for $Cu_{12}Cr$ and 0-300 cm^{-1} for $Ag_{12}Cr$. These finding suggest an extension of the observed wavelength range compared to the pure clusters Cu_{13} (0 – 300 cm^{-1}) and Ag_{13} (0-200 cm^{-1}. Conversely, the IR spectral peaks of Au_{13} and $Au_{12}Cr$ clusters are situated within the wavelength range of 0-260 cm^{-1}. This is in agreement with the vibration frequency of 3*d*, 4*d* and 5*d* 13-atom metal clusters [29].

The IR spectrum of Cu_{13} clusters displays 11 distinct bands corresponding to three primary vibrational modes: i) the calculated vibrational frequency of Cu_{13} was 75 cm^{-1}, while other studies reported a frequency of 60 cm^{-1} [30]. This band is assigned to the bending mode involving two triangular Cu atoms around the Cu_7 framework. Additionally, the wavelengths 109 cm^{-1}, 116 cm^{-1}, and 137 cm^{-1} are associated with the bending mode of a single Cu atom within the Cu_{13} cluster. ii) The asymmetric stretching mode of Cu-Cu in the Cu_{13} framework is characterized by the frequencies of 90 cm^{-1}, 152 cm^{-1}, 176 cm^{-1}, 206 cm^{-1}, 233 cm^{-1}, 265 cm^{-1}, respectively. This values are in good agreement with the experimental value of Cu-Cu vibration of 265 cm^{-1} [31]. iii) Conversely, an opposite trend is observation at the peak if 254 cm^{-1}, which is signifies the

symmetric stretching mode of Cu-Cu vibration in the Cu_{13} clusters. It is noteworthy that the IR spectra of $Cu_{12}Cr$ cluster show significant differences. The spectra exhibit a noticeable shift towards longer wavenumber and are relatively simple, featuring a very high intense peak at 348 cm^{-1}. This peak corresponds to the Cr-Cu symmetric stretching vibrational mode in the Cu_{12} framework. Similarly to the $Cu_{12}Cr$ and Cu_{13} clusters, the IR spectra of $Ag_{12}Cr$ and Ag_{13} clusters display analogous characteristic. The bending vibrational mode involving two triangular Ag atoms around Ag_7 framework is observed at a low frequency of 43 cm^{-1}. In the meantime, the wavelength 112 cm^{-1} is assigned for bending vibrational mode of an Ag in Ag_{13}. The symmetric stretching vibrational mode of Ag-Ag in Ag_{13} are characterized by frequencies of 51 cm^{-1}, 151 cm^{-1}. In contrast, the asymmetric stretching vibrational mode of Ag-Ag in Ag_{13} are represented by wavelengths of 84 cm^{-1}, 93 cm^{-1}, 135 cm^{-1}, 164 cm^{-1}, while asymmetric stretching mode of triangle Ag_3 in Ag_{13} is noted at 172 cm^{-1}. This picture show good agreement for the neutral Ag-Ag dimer vibration at a frequency of 145 cm^{-1} [32]. Unlike the $Cu_{12}Cr$, the IR spectra of $Ag_{12}Cr$ clusters shows two peaks. The lower intensity peak, corresponding to a frequency approximately118 cm^{-1}, is associated with the asymmetric stretching of Cr-Ag bonds within Ag_{12} framework. Conversely, the higher intensity peak is attributed to the symmetric stretching of Cr-Ag in the same framework.

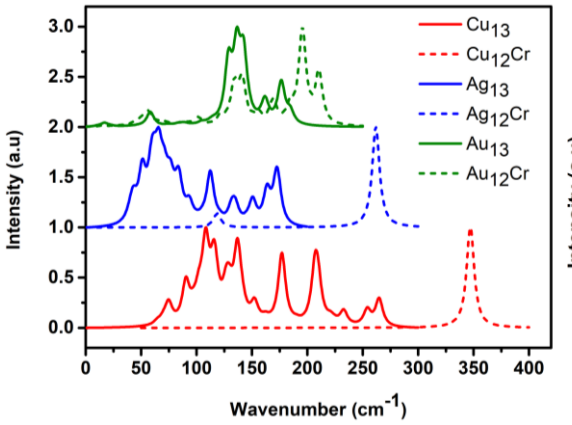

Figure 2. *IR spectra for M_{13} and $M_{12}Cr$ (M = Cu, Ag, and Au) clusters. The red, blue, and olive lines represent the IR spectrum of pure copper, silver, and gold clusters (solid lines) and their Cr-dopant (short dash), respectively.*

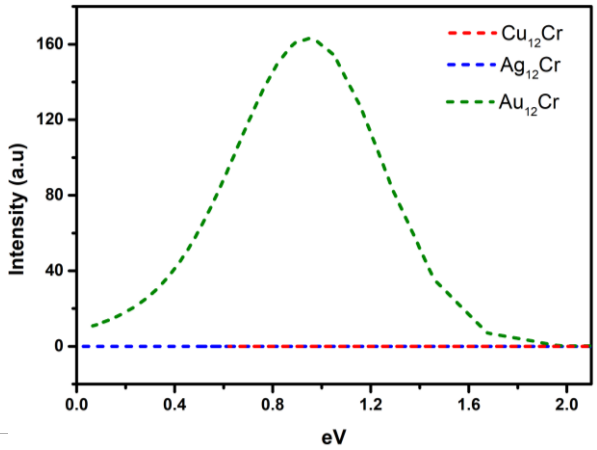

Figure 3. *UV-Vis spectra for $M_{12}Cr$ (M = Cu, Ag, and Au) clusters. The red, blue, and olive short dash represent the UV-Vis spectrum of $Cu_{12}Cr$, $Ag_{12}Cr$, and $Au_{12}Cr$ clusters, respectively.*

As illustrated in Figure 2, the IR spectrum of truncated cone A_{13} reveals six peaks characteristic of three specific types of vibrations: at low frequency corresponding to 16 cm^{-1}, which is associated with the bending vibrational mode of two Au atom at the corners. While the peaks at 56 $cm^{-1,}$ is assigned symmetric stretching of Au-Au in Au_{13} clusters, the peaks of 126 cm^{-1} and 140 cm^{-1} are associated with the asymmetric stretching of Au-Au bonds. In contrast, the wavelengths of 134 cm^{-1}, 160 cm^{-1}, and 174 cm^{-1} characterize the asymmetric stretching of triangular Au_3 on Au_{10}. Considering the distorted cone shaped $Au_{12}Cr$ spectrum, it can be observed two asymmetric stretching modes of Cr-Au bonds at high frequencies: ~210 cm^{-1} and ~227 cm^{-1}. The peaks at ~110 cm^{-1}, ~141 cm^{-1} and ~163 cm^{-1} are assigned to the symmetric stretching of Au-Au bonds. Conversely, the asymmetric stretching modes of Au-Au bonds are assigned at ~ 64 cm^{-1}, ~110 cm^{-1}, ~130 cm^{-1}, ~152 cm^{-1} and ~177 cm^{-1}. In other words, transition metal atoms play an important role in the formation of geometric structures and characteristic vibrations within doped clusters. Insights gained from infrared spectral analysis provide significant information regarding bonding characteristics, properties, and potential applications of these clusters in the fields of physical chemistry and materials science.

To investigate the adsorption properties of $M_{12}Cr$ clusters for comparison, time-dependent density functional theory (TD-DFT) was performed. Notably, there are currently no publications regarding the UV-Vis spectra of the $M_{12}Cr$ clusters (M = Cu, Ag, and Au). Therefore, these findings provide a valuable reference point for future experimental investigations. The UV-Vis spectra of $M_{12}Cr$ are plotted in Figure 3. While the UV-Vis spectra of $Cu_{12}Cr$ and $Ag_{12}Cr$ clusters exhibit no observable absorption peaks, the UV-Vis spectrum of $Au_{12}Cr$ cluster is distinguished by an adsorption band with an absorption maximum of 1270 nm (0.976 eV), corresponding to a vibrational intensity of 0.0037 a.u. This absorption peak is associated with the electronic transition from HOMO-125 to LUMO, as illustrated in Figure 4.

In Figure 4, one can observe both the HOMO-125 and LUMO of $Au_{12}Cr$ cluster are primarily formed from the d orbital of Cr atom. This phenomenon can be elucidated by examining the electronic configurations of the $M_{12}Cr$ clusters. Doping a Cr atom into metal clusters creates a hybridization framework involving delocalized electrons and localized electrons in these clusters. The delocalized electrons primarily contribute to the stability of the clusters, whereas the localized electrons in the 3*d* orbitals of Cr play in pivotal role in determining magnetic, catalytic, and optical properties [5], [6], [33]. For $Cu_{12}Cr$ and $Ag_{12}Cr$, there is a strong hybridization between all the valence electrons of Cr atom ($3d^5 4s^1$) with twelve valence electrons of Cu_{12}/Ag_{12} host.

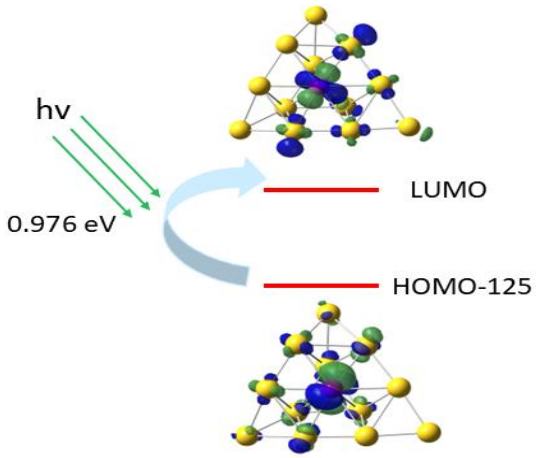

Figure 4. *Molecular orbital diagrams for electronic transition (eV) with an image of atomic orbital components contributing to each transition of $Au_{12}Cr$ cluster*

This interaction results in a close electron configuration consisting of 18 electrons, corresponding to close shell of $1S^2 1P^6 1D^{10}$. In contrast, for $Au_{12}Cr$ cluster, only a portion of the Cr valence electrons (one from the $4s^1$ and one electron of $3d^5$ orbitals) participates in the hybridization, forming the free electron configuration of $1S^2 1P^6 1D^6$. The remaining four valence electrons of Cr are localized in it 3*d* orbital. Consequently, the electronic configuration is formed as $1S^2 1P^6 1D^6 3d^4_{Cr\uparrow}$. In other words, in addition to the impact of geometric structure, the unpaired valence electrons of the 3*d*-transition metal atom play a crucial role in the adsorption capacity of the clusters.

4. Conclusion

The vibrational infrared spectra and absorption spectra of the ground-state structures of M_{13} and $M_{12}Cr$ (M = Cu, Ag, and Au) clusters have been investigated using density functional theory and time-dependent density functional theory approaches. We utilized the BP86 functional in conjunction with cc-pVTZ-pp and cc-pVTZ basis sets for M and Cr atoms, respectively. Our findings demonstrate that the IR spectra reveal significant variation in the vibrational modes between the pure M_{13} clusters and the $M_{12}Cr$ clusters. UV-Vis spectral analysis indicated the absence of absorption signals from both $Ag_{12}Cr$ and $Cu_{12}Cr$ clusters. Conversely, a distinct absorption peak at a wavelength of 1270 nm (0.976 eV) was observed for $Au_{12}Cr$ cluster. This phenomenon can be attributed to strong hybridization between valence electrons of Cr and those of the host systems. The icosahedral $Cu_{12}Cr$ and $Ag_{12}Cr$ singlet clusters, all five valences electrons of Cr interact with twelve valence electrons of Cu/Ag, forming a fully electron shell of clusters with the configuration $1S^2 1P^6 1D^{10}$. Conversely, the cone-like $Au_{12}Cr$ quintet clusters, only two valence electrons of Cr contribute to the electron shell, while the remaining four

electrons localize in the 3*d*-Cr, resulting in an electronic configuration of $1S^2 1P^6 1D^6 3d^4_{\uparrow}$. These studies results provide fundamental insights into the vibrational characteristics and how structural and electronic configurations influence their optical characteristics, laying the groundwork for further theoretical and experimental investigations.

Acknowledgments

This research was financially supported by National Foundation of Science and Technology Development (NAFOSTED) under the grant number 103.01-2021.109.

REFERENCES

[1] S. Khanna and P. Jena, "Assembling crystals from clusters," *Physical Review Letters*, vol. 69, no. 11, 1992, Art. no. 1664.

[2] S. Khanna and P. Jena, "Atomic clusters: Building blocks for a class of solids," *Physical Review B*, vol. 51, no. 19, 1995, Art. no. 13705.

[3] A. C. Jr and S. Khanna, "Clusters, superatoms, and building blocks of new materials," *The Journal of Physical Chemistry C*, vol. 113, no. 7, pp. 2664-2675, 2009.

[4] H. Haberland, *Clusters of atoms and molecules: theory, experiment, and clusters of atoms*, Springer Science & Business Media, Hellmut Haberland (Ed), 2013.

[5] T. L. Ngo, T. M. Nguyen, D.D. La, M. T. Nguyen, S.T. Ngo, T. C. Ngo, V. D. Nguyen, T. T. Phung, and T. T. Nguyen, "DFT investigation of Au_9M^{2+} nanoclusters (M= Sc-Ni): The magnetic superatomic behavior of Au_9Cr^{2+}," *Chemical Physics Letter*, vol. 793, 2022, Art. no. 139451.

[6] T. M. Nguyen, T. L. Ngo, T. C. Ngo, M. T. Nguyen, S. T. Ngo, T. T. Phung, V. D. Nguyen, and T. T. Nguyen, "Systematic Investigation of the Structure, Stability, and Spin Magnetic Moment of CrM_n Clusters (M= Cu, Ag, Au, and n= 2–20) by DFT Calculations," *ACS omega*, vol. 6, no. 31, pp. 20341-20350, 2021.

[7] M. T. Nguyen, T. M. Nguyen, H. T. Pham, T. C. Ngo, and T. T. Nguyen, "Ultimate Manipulation of Magnetic Moments in the Golden Tetrahedron Au_{20} with a Substitutional 3*d* Impurity," *The Journal of Physical Chemistry C*, vol. 122, no. 28, pp. 16256-16264, 2018.

[8] M. T. Nguyen, T. C. Ngo, H. T. Pham, and T. T. Nguyen, "$Au_{19}M$ (M= Cr, Mn, and Fe) as magnetic copies of the golden pyramid," *Scientific Reports,* vol. 7, no. 1, 2017, Art. no. 16086.

[9] R. Xiong, D. Die, L. Xiao, Y.-G. Xu, and X.-Y. Shen, "Probing the structural, electronic, and magnetic properties of Ag_nV (n= 1–12) clusters," *Nanoscale Research Letters*, vol. 12, pp. 1-12, 2017.

[10] M. Zhang, H. Zhang, L. Zhao, Y. Li, and Y. Luo, "Low-Energy Isomer Identification, Structural Evolution, and Magnetic Properties in Manganese-Doped Gold Clusters $MnAu_n$ (n = 1–16)," *The Journal of Physical Chemistry A*, vol. 116, no. 6, pp. 1493-1502, 2012.

[11] V. M. Medel, Arthur C. Reber, V. Chauhan, P. Sen, A. M. Köster, P. Calaminici, and S. N. Khanna, "Nature of valence transition and spin moment in Ag_nV^+ clusters," *Journal of the American Chemical Society*, vol. 136, no. 23, pp. 8229-8236, 2014.

[12] Y. S. Xu, D. Die, and B. X. Zheng, "Growth pattern and electronic and magnetic properties of Cr-doped silver clusters," *Journal of Computational Chemistry*, vol. 44, no. 29, pp. 2284-2293, 2023.

[13] W. Li and F. Chen, "Effect of Cu-doped site and charge on the optical and magnetic properties of 55-atom Ag cluster: A density functional theory study," *Computational materials science*, vol. 81, pp. 587-594, 2014.

[14] T. L. Ngo, T. M. Nguyen, D. D. La, S. T. Ngo, M. T. Nguyen, V. D. Nguyen, and T. T. Nguyen , "Exploring hydrogen adsorption on nanocluster systems: Insights from DFT calculations of Au_9M^{2+} (M= Sc-Ni)," *Chemical Physics Letter*, vol. 831, 2023, Art. no. 140838.

[15] T. L. Ngo, T. M. Nguyen, T. C. Ngo, T. H. V. Phung, D. D. La, M. T. Nguyen, S. T. Ngo, and T. T. Nguyen, "Density Functional Study of Size-Dependent Hydrogen Adsorption on Ag_nCr (n= 1–12) Clusters," *ACS omega*, vol. 7, no. 42, pp. 37379-37387, 2022.

[16] M. Szalay, D. Buzsáki, J. Barabás, E. Faragó, E. Janssens, L. Nyulászi, and T. Höltzl, "Screening of transition metal doped copper clusters for CO_2 activation," *Physical Chemistry Chemical Physics*, vol. 23, no. 38, pp. 21738-21747, 2021.

[17] W. Li, H. Feng, and R. Shang, "First Principle Study on Structural, Electronic, Magnetic, and Optical Properties of Co-Doped Middle Size Silver Clusters," *Molecules*, vol. 29, no. 11, 2024, Art. no. 2670.

[18] W. Ma and F. Chen, "Optical and electronic properties of Cu doped Ag clusters," *Journal of alloys and compounds*, vol. 541, pp. 79-83, 2012.

[19] V. Kaydashev, P. Ferrari, C. Heard, E. Janssens, R. L. Johnston, and P. Lievens, "Optical absorption of small palladium-doped gold clusters," *Particle & Particle Systems Characterization*, vol. 33, no. 7, pp. 364-372, 2016.

[20] M. Frisch, G. W. Trucks, H. B. Schlegel, M. J. Frisch, G. W. Trucks, H. B. Schlegel, G. E. Scuseria, M. A. Robb, J. R. Cheeseman, G. Scalmani, V. Barone, B. Mennucci, and G. A. Petersson, *Gaussian 09, Revision a. 02, 200*, Gaussian, Inc., Wallingford, CT, vol. 271, 2009.

[21] P. Hohenberg and W. Kohn, "Inhomogeneous electron gas," *Physical review*, vol. 136, no. 3B, 1964, Art. no. B864.

[22] O. Ingólfsson, U. Busolt, and K.-i. Sugawara, "Energy-resolved collision-induced dissociation of Cu_n^+ (n= 2–9): Stability and fragmentation pathways," *The Journal of Chemical Physics*, vol. 112, no. 10, pp. 4613-4620, 2000.

[23] Y.-R. Luo, *Comprehensive handbook of chemical bond energies*. CRC press, 2007.

[24] S. F. Li, S. Zenlun, H. Shuli, X. Xinlian, F. Wang, Q. Sun, J. Yu, and Z. X. Guo, "Role of Ag doping in small transition metal clusters from first-principles simulations," *The Journal of chemical physics*, vol. 131, no. 18, pp. 184301-18410, 2009.

[25] T. L. Ngo, V. D. Nguyen, T. M. Nguyen, T. T. Phung, D. T. Nguyen, and T. T. Nguyen, "Insights into the structural, electronic and magnetic properties of gold clusters: Comparison between $Au_{12}Cr$ and $Au_{12}Mo$ clusters," *Communications in Physics*, vol. 34, no. 4, pp. 389-398, 2024.

[26] S. Bhattacharyya, T. T. Nguyen, J. D. Haeck, K. Hansen, P. Lienvens, and E. Janssens, "Mass-selected photodissociation studies of $AlPb_n^+$ clusters (n= 7–16): Evidence for the extraordinary stability of $AlPb_{10}^+$ and $AlPb_{12}^+$," *Physical Review B—Condensed Matter and Materials Physics*, vol. 87, no. 5, 2013, Art. no. 054103.

[27] T. M. Nguyen, S. T. Ngo, P. Lienvens, E. Janssens, and T. T. Nguyen, "Photofragmentation Patterns of Cobalt Oxide Cations $Co_nO_m^+$(n= 5–9, m= 4–13): From Oxygen-Deficient to Oxygen-Rich Species," *The Journal of Physical Chemistry A*, vol. 124, no. 37, pp. 7333 - 7339, 2020.

[28] T. T. Nguyen, E. Janssens, and P. Lienvens, "Dopant dependent stability of Co_nTM^+ (TM= Ti, V, Cr, and Mn) clusters," *Applied Physics B*, vol. 114, pp. 497-502, 2014.

[29] M. J. Piotrowski, P. Piquini, and J. L. Da Silva, "Density functional theory investigation of 3*d*, 4*d*, and 5*d* 13-atom metal clusters," *Physical Review B,* vol. 81, no. 15, 2010, Art. no. 155446.

[30] C. C. Quevedo, C. E. B. Garcia, E. P. Sotelo, E. R. Chaparro, G. M. Guajardo, J. Manuel, Q. Castillo, A. L. Flores, T. Gaxiola, S. J. Castillo, A. V. Espinal, and J. L. Cabellos , "Relative abundances and enantiomerization energy of the chiral Cu_{13} cluster at finite temperature," *Condensed Matter*, vol. 2109, 2021, Art. no. 03981.

[31] C. W. Bauschlicher, S. P. Walch, and P. E. Siegbahn, "On the nature of the bonding in Cu_2," *The Journal of Chemical Physics,* vol. 76, no. 12, pp. 6015-6017, 1982.

[32] J. Jin, M. Grellmann, and K. R. Asmis, "Nuclear quantum dynamics on the ground electronic state of neutral silver dimer ^{107}Ag ^{109}Ag probed by femtosecond NeNePo spectroscopy," *Phys. Chem. Chem. Phys.,* vol. 25, no. 36, pp. 24313-24320, 2023.

[33] T. L. Ngo, "Research on the physical interaction between delocalized and localized electrons in Au_9M^{2+} (M = Sc-Ni) and Ag_nCr (n = 2-12) alloy nanoclusters systems using density functional theory," PhD Thesis, Graduate University of Science and Technology, 2024.